Body-worn Fully-Passive Wireless Analog Sensors for Biopotential Measurement Through Load Modulation

Sergi Consul-Pacareu, David Arellano, and Bashir I. Morshed

Electrical and Computer Engineering, The University of Memphis, Memphis, TN 38152

***Abstract*— Fully-passive wireless and disposable body-sensors are promising for unobtrusive monitoring of physiological signals at natural settings. We present a new type of wireless analog passive sensor (WAPS) based on resistive damping, which can be used for biopotential sensing. The resistive WAPS operates by modulating the amplitudes of the incident RF signal, and composes of a loop antenna, a tuning capacitor, and a MOSFET (an additional biasing resistance is used in one variation). The scanner transmits carrier RF signal at $13.34MHz$ and the load modulated signal is captured with the signal analyzer. The envelope of the modulated signal correlates with the biopotential being sensed. Both enhancement and depletion MOSFETs are demonstrated, where the earlier demonstrated superior performance. The sensitivity can be as low as 10 mV, suitable for ECG and EMG physiological signal capture. The transmission power were 0 dBm while the co-axial separation between antennas were 21.5 mm. The results show that the proposed WAPS can be used to develop disposable biopotential sensor suitable for body-worn physiological signal monitoring system.**

I. Introduction

As the number of sensors in a body-worn system increases, wired sensors eventually becomes complex and unmanageable. Traditional wireless sensors are also not very effective due to the requirement of battery that restricts size, cost and usability. Fully-passive sensors can be designed as body-worn sensors, and can collect physiological signals unobtrusively [1]-[3]. There can be two classes of fully-passive sensors: wireless digital passive sensor (WDPS) and wireless analog passive sensor (WAPS). WDPS usually contain an ASIC chip that receives power from the scanner, turns on the circuitry, collects signal or data, and then wirelessly retransmits the digitized signal or code. WDPS can collect analog signals by sampling the analog data with data acquisition chips [4], [5]. WAPS, however, does not contain any digital chip, rather transmits analog signals directly. WAPS based on varactor and Surface Acoustic Wave (SAW) resonator has been demonstrated for biopotential signal capture [6]-[9]. As these WAPS uses LC resonators, there is a shift of the resonance frequency based on the captured signals [8], [9]. For delayed backscattering, the SAW delay line is used that aids in capturing the backscattered signal [7], [10].

In this paper, we demonstrate the feasibility of a new resistive based WAPS for biopotential capture. Here, the passive sensor is an RLC resonator with damping factor Q. The biopotential signal causes a variation of the resistive load, altering the damping factor that modulates the carrier RF signal accordingly. This amplitude modulation can be captured at the signal analyzer with an envelope detector. Such body-worn passive sensors can allow remote capture of data such as Electroencephalography (ECG) and Electromyography (EMG). These WAPS are very simple, low cost, low component count, and can be disposable.

II. Theory

From the passive sensor side, secondary coil sensor impedance is equal to Eq.1 [11].

$$Z_{Sensor}(w) = \left(jwL_2 || \left(\frac{1}{jw(C_5 + C_6)} \right) || R_L \right) \quad (1)$$

From the primary, for a mutual inductance of M, the sensor impedance can be seen as following [9]:

$$X_{Sen}(w) = \left(\frac{(wM)^2}{Z_{Sen}(w)} \right) \quad (2)$$

The impedance encountered by the signal analyzer is:

$$Z_{Rec}(w) = \left(X_{Sen}(w) + jwL_1 || \frac{1}{jw(C_4 + C_3 + C_2 + C_1)} || R_1 \right) \quad (3)$$

Eq.3 shows that a change in load resistance, R_L, in the sensor will cause a change in the amplitude of the received signal, thus amplitude modulating the carrier signal.

III. Hardware Description

For prototype development, two identical sized boards has been designed Cadence PSPICE tool (Cadence Design Systems, Inc., San Jose, CA, USA). Fig. 1 shows the schematic for the scanner device, and three schematics for various WAPS sensor design. The antenna design was based on the designs from [12]. The scanner board has two SMA connectors, one for the carrier input V_1, which delivers carrier signals at $13.34MHz$, and the other one for the signal analyzer. The capacitor C_{ss} is used to match the antenna to 50Ω. Another capacitor C_{sp} is used to adjust the resonant frequency with the loop antenna (L_s) which is designed as a planar inductor. The damping resistor (R_{sp}) is used to lower Q. The passive sensor has a matching coil

L_i and a capacitor C_i to tune the antenna at the resonant frequency. In Fig. 1b, a resistive load R_L is shown that represents a resistive transducer to convert a physical signal to a correlated resistance value for remote capturing of signal. In Fig. 1c and 1d, the MOSFETs are used to convert input voltage (V_s) to a correlated resistive variation of R_{SD}. The former schematic has no biasing, while the latter has a resistive biasing path.

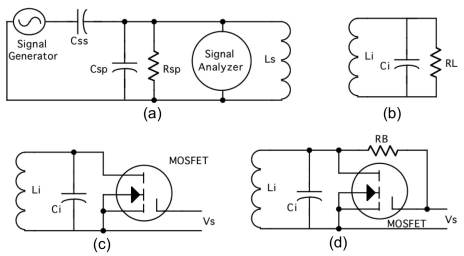

Fig. 1. (a) Schematic of the scanner for WAPS. (b) Schematic of the transducer based WAPS. (c) Schematic of MOSFET based WAPS for biopotential sensing. (d) Alternative schematic of MOSFET based WAPS for biopotential sensing.

Printed Circuit Boards (PCBs) were designed using Cadence Allegro SPB 16.6 (Cadence Design Systems Inc., San Jose, CA, USA). The sensor and scanner boards are of identical in size measuring 6.89 cm $\times$ 4.19 cm. The PCBs were fabricated by Advanced Circuits (Aurora, CO, USA). The populated sensor and scanner devices weigh 9.07g and 11.75g, respectively. The test fixture kept the boards in parallel at a co-axial position (Fig. 2).

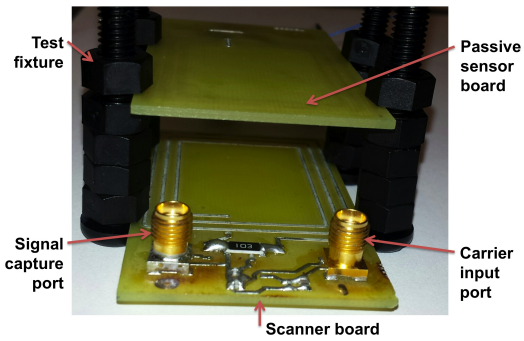

Fig. 2. The test setup for the scanner and the sensor at co-axial parallel positions where separations between coils can be altered.

IV. Method

A DSA1030-TG3 (Rigol Technologies Inc,. Beijing, China) spectrum analyzer measures the reflected signal from the sensor in the frequency domain. The Tracking Generator on this device is also used to sweep signals with RBW = VBW = 1KHz, and Gauss Filter. For each varying separation, the resonant is determined (which varies due to parasitic) and then set as the carrier frequency. The signals scan at -20dBm and then -15dBm with a 3MHz span about the center frequency. For temporal measurements, a Wavetek 5135A (Aeroflex Inc., Plainview, New York, USA) frequency synthesizer generates a 13.34MHz signal. The output is connected to a DSO-X 2024A (Agilent Technologies Inc., Santa Clara, CA, USA) Oscilloscope with AC coupling, with settings of AC coupled, 1mV/div, Peak Detect as acquisition mode, and ASCII X-Y as output option. Data from the oscilloscope is saved as a .cvs file, and then complied and plotted in Matlab. The scanner and the passive sensor maintained a separation distance of 5 to 50 mm at co-axial position for all measurements by using the testing fixture as shown in Fig. 2.

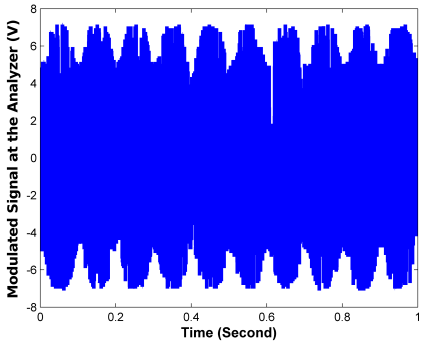

Fig. 3. Load modulated signal captured at the signal analyzer with 0 dBm Tx power and 21.5mm separation. The amplitude modulated envelope correlates to V_s (2Vpp, 10 Hz).

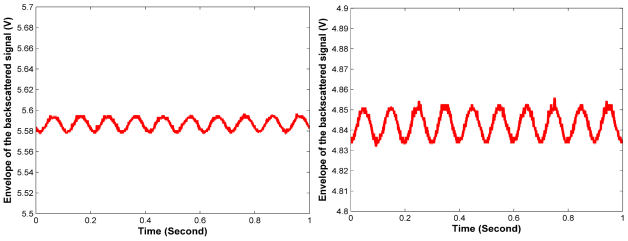

Fig. 4. The positive envelope of the modulated signal for V_s = 200mV (left) and V_s = 10mV (right), captured using a WAPS with depletion MOSFET.

V. Results

Fig. 3 shows the received amplitude modulated signal for the application of V_s = 2 V at the input of the MOSFET as depicted in Fig. 1c. The amplitude of the detected signal corresponds to V_s. The transmission power were 0 dBm. Fig. 4 shows the positive envelope of the captured signal at the spectrum analyzer for 200 mV and 10 mV input signals (V_s) captured with Fig. 1d schematic.

Fig. 5 shows the voltage response of WAPS for the schematic in Fig. 1c with an enhancement MOSFET. The region near the origin is amplified in the inset. A set of trend lines are shown that is based on the second order polynomials. Fig. 6 shows the voltage response of WAPS

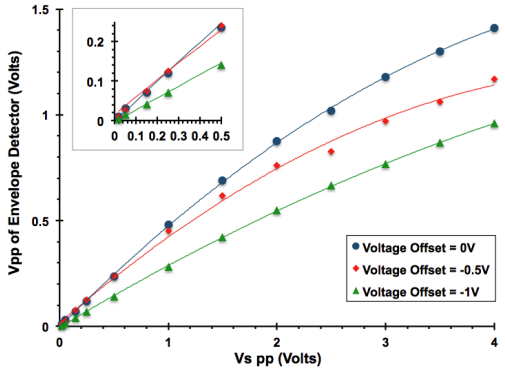

Fig. 5. Voltage response of WAPS for schematic in Fig. 1c with an enhancement MOSFET along with second order polynomial trend lines.

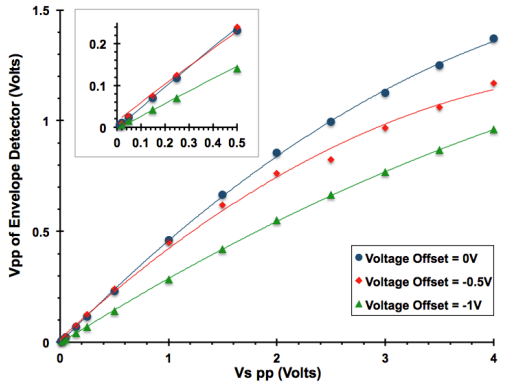

Fig. 6. Voltage response of WAPS for schematic in Fig. 1d with an enhancement MOSFET along with second order polynomial trend lines.

for the schematic in Fig. 1d with an enhancement MOSFET. Similarly, Fig. 7 shows the voltage response of WAPS for the schematic in Fig. 1c with a depletion MOSFET. A set of trend lines are shown that is based on the third order polynomials. Fig. 8 shows the corresponding voltage response for the schematic in Fig. 1d.

VI. Conclusions

In this paper, we show that WAPS can capture biopotentials remotely. The WAPS successfully captured potentials as low as 10 mV over 21.5 mm separation, demonstrating the feasibility to develop body-worn WAPS for ECG or MEG signals, while the scanner can be wearable. The system is suitable for disposable sensors due to the low cost and low component count of the passive sensors. The results show the promise of developing a body-sensor-network with multiple passive sensors accessed simultaneously using frequency-multiplexing technique.

References

[1] Y. M. Chi, T. Jung, and G. Cauwenberghs, Dry-contact and noncontact biopotential electrodes: methodological review, IEEE Reviews in Biomedical Engineering, vol. 3, pp. 106-119, 2010.

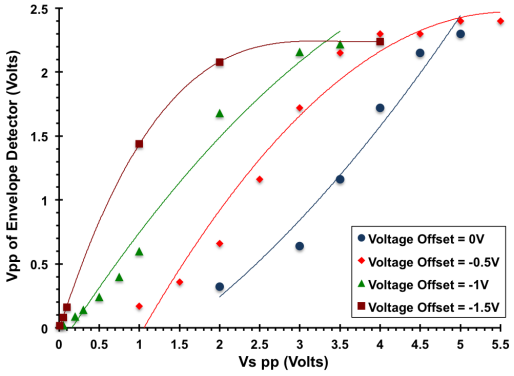

Fig. 7. Voltage response of WAPS for schematic in Fig. 1c with a depletion MOSFET along with third order polynomial trend lines.

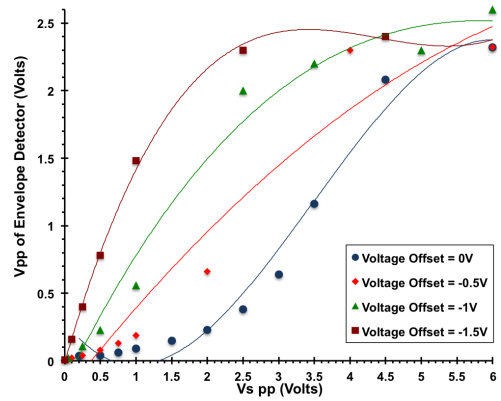

Fig. 8. Voltage response of WAPS for schematic in Fig. 1d with a depletion MOSFET along with third order polynomial trend lines.

[2] A. Sabban, Comprehensive study of printed antennas on human body for medical applications, Intl. J. Advance in Medical Sci., vol. 1, no. 1, pp. 1-10, 2013.
[3] A. Dementyev, and J. R. Smith, A wearable UHF RFID-based EEG system, IEEE Intl. Conf. RFID, pp. 1-7, 2013.
[4] M. Sawan, Y. Hu, and J. Coulombe, "Wireless smart implants dedicated to multichannel monitoring and microstimulation," IEEE Circuits and Systems Magazine, vol. 5, no. 1, pp. 21-39, 2005.
[5] R. Bashirullah, Wireless implants, IEEE Microwave Magazine, pp. S14-S23, Dec. 2010.
[6] Z. Popovic, E.A. Falkenstein, D. Costinett, and R. Zane, Low-power far-field wireless powering for wireless sensors, Proc. IEEE, vol. 101, no. 6, pp. 1397-1409, 2013.
[7] W. Luo, Q. Fu, J. Deng, G. Yan, D. Zhou, S. Gong, Y. Hu, An integrated passive impedance-loaded SAW sensor, Sensors and Actuators B: Chemical, vol. 187, pp. 215-220, 2013.
[8] H.N. Schwerdt, *et al.*, A fully-pasive wireless microsystem for recording of neuropotentials using RF backscattering methods, J. Microelectromech Syst., vol. 20, no. 5, pp. 1119-1130, 2011.
[9] J. Riistama, E. Aittokallio, J. Verho, and J. Lekkala, Totally passive wireless biopotential measurement sensor by utilizing inductively coupled resonance circuits, Sensors and Actuators A, vol. 157, pp. 313321, 2010.
[10] W. Luo, Q. Fu, J. Deng, G. Yan, D. Zhou, S. Gong, Y. Hu, "An integrated passive impedance-loaded SAW sensor," Sensors and Actuators B: Chemical, vol. 187, pp. 215-220, 2013.
[11] K. Finkenzeller, The RFID Handbook, John Wiley and Sons, 2003.
[12] J.A. Goulbourne, "HF Antenna Cookbook", Texas Inst., 2001.